



## ORIGINAL ARTICLE

# Priority Switches in Visual Working Memory are Supported by Frontal Delta and Posterior Alpha Interactions

Ingmar E.J. de Vries , Joram van Driel, Merve Karacaoglu and Christian N.L. Olivers

Department of Experimental and Applied Psychology, Faculty of Behavioural and Movement Sciences, Vrije Universiteit Amsterdam, Van der Boechorststraat 1, 1081BT Amsterdam, Netherlands

Address correspondence to email: Ingmar E.J. de Vries. Email: [i.e.j.de.vries@vu.nl](mailto:i.e.j.de.vries@vu.nl)  [orcid.org/0000-0002-0174-7320](https://orcid.org/0000-0002-0174-7320)

## Abstract

Visual working memory (VWM) distinguishes between representations relevant for imminent versus future perceptual goals. We investigated how the brain sequentially prioritizes visual working memory representations that serve consecutive tasks. Observers remembered two targets for a sequence of two visual search tasks, thus making one target currently relevant, and the other prospectively relevant. We show that during the retention interval prior to the first search, lateralized parieto-occipital EEG alpha (8–14 Hz) suppression is stronger for current compared with prospective search targets. Crucially, between the first and second search task, this difference in posterior alpha lateralization reverses, reflecting the change in priority states of the two target representations. Connectivity analyses indicate that this switch in posterior alpha lateralization is driven by frontal delta/low-theta (2–6 Hz) activity. Moreover, this frontal low-frequency signal also predicts task performance after the switch. We thus obtained evidence for large-scale network interactions underlying the flexible shifting between the priority states of multiple memory representations in VWM.

**Key words:** cognitive control, cross-frequency-coupling, EEG, neural oscillations, visual attention

## Introduction

When we perform sequences of various tasks, we flexibly attend to incoming information relevant for their completion. Visual working memory (VWM) plays an important role in selecting information from the visual input that is important for our behavioral goals, by pre-activating task-relevant target representations, which then bias selection towards matching visual stimuli (Duncan and Humphreys 1989; Bundesen 1990; Wolfe 1994; Desimone and Duncan 1995; Olivers et al. 2006). However, VWM not only serves current, but also future perceptual goals. It also maintains representations that become

prospectively relevant, and that therefore should be shielded from the current perceptual input. Consequently, it has been proposed that working memory representations are maintained in different states depending on their current versus prospective relevance in multi-task paradigms (Oberauer 2002; Olivers et al. 2011; Lewis-Peacock et al. 2012; Stokes 2015).

Performing such task sequences means that at some point in time, the representation that was initially relevant needs to be abandoned, and the one that was prospectively relevant now needs to become current. Little is known about such switches in priority within VWM, and what drives them. In the

present study, we investigated the oscillatory signals that underlie the switch from current to prospective perceptual goals. First, amplitude modulations of posterior alpha (8–14 Hz) oscillations might reflect changes in the relative priority of representations. There is a large body of evidence indicating that alpha lateralization supports the selection of task-relevant information for further processing, as has been shown both for external selection of relevant stimuli by means of visual attention (Sauseng et al. 2005b; Romei et al. 2010; Spaak et al. 2015), and for internal selection of information maintained within VWM (Zumer et al. 2014; Myer et al. 2015b; Schneider et al. 2015, 2016; van Ede 2017; van Ede et al. 2017). Recently, we have shown that posterior alpha lateralization is also sensitive to the temporal order in which multiple VWM representations will become task-relevant (de Vries et al. 2017). During maintenance, alpha lateralization was stronger for items that were relevant for an upcoming visual search task, compared with items that were remembered for a second search task that only happened after the first search task was completed. In the present study, we assessed how such goal-driven alpha lateralization alters when observers switch from one search task to the next. After the first search task, the former target representation is no longer task-relevant, and can be dropped. Moreover, priority should be assigned to the heretofore prospective representation. We hypothesized that these operations would be reflected in a reversal of alpha lateralization. First, we replicate our previous finding by showing that the prioritized VWM state is reflected in hemisphere-specific alpha suppression during encoding and initial maintenance. Importantly, we then also demonstrate that goal-driven prioritization and de-prioritization of memory representations is tracked by hemisphere-specific alpha suppression and alpha enhancement, respectively.

Second, we sought to uncover the control signal that is driving any switch-related alpha modulations within VWM as a function of changing task goals. Such changes can be considered a form of task switching, and are therefore likely to involve top-down, cognitive control mechanisms emanating from frontal regions (Fuster 2001; Miller and Cohen 2001; Monsell 2003). Frontal cortical areas have indeed been shown to mediate synchronization in posterior visual areas during attention (Marshall et al. 2015; Paneri and Gregoriou 2017) and VWM tasks (Lara and Wallis 2015; van Driel et al. 2017). Specifically, evidence points to frontal oscillatory activity in the lower frequency range (delta-to-theta; 2–6 Hz) as a key mechanism for top-down control of endogenous attentional selection (Jensen and Tesche 2002; Onton et al. 2005; Sauseng et al. 2005a; 2010; Daitch et al. 2013; Aleksehchuk et al. 2016; Helfrich and Knight 2016; Johnson et al. 2017). Moreover, connectivity between frontal low-frequency oscillations and posterior alpha oscillations has been observed during top-down control of visual perception (Helfrich and Knight 2016; Helfrich et al. 2017). Here, we provide novel evidence that transiently coupled large-scale functional networks between frontal and posterior regions underlie the top-down control of goal-driven priority switches within VWM, as reflected in cross-frequency coupling between frontal delta and lateralized posterior alpha oscillations. Moreover, we show that these frontal delta oscillations predict post-switch behavioral performance.

## Materials and Methods

### Subjects

In an initial selection and training session, 32 healthy human subjects with normal or corrected-to-normal vision performed

the experimental task without EEG, after which only those with sufficient performance (above 70% accuracy, 22 subjects: ages 19–32 years, 15 female) were selected for the EEG experiment. All subjects participated for course credit or monetary compensation. Two subjects were removed due to bad performance (i.e., below 70% accuracy) in the EEG session, leaving 20 subjects for all analyses. The procedures used were conducted in accordance with the Declaration of Helsinki and were positively reviewed by the faculty's Scientific and Ethical Review Board. Written informed consent was obtained.

### Task Design

This study used an adapted version of the design with similar parameters as described in de Vries et al. (2017). For clarity and completeness, the full experimental design and parameters are described here. Each trial consisted of 2 consecutive VWM-guided visual search tasks (Fig. 1A). A trial started with a fixation cross on a gray background for a duration of 1400–1800 ms (randomly jittered), followed by a memory display in which 4 colored circles surrounded the fixation cross (left, right, top, and bottom) for 400 ms. Two of these colors were to be remembered for the two subsequent search tasks, as indicated by their black outlines: the color with a dashed outline was the target for the first search task, and thus served as the template for that search task, while the color with a dotted outline was the target for the second search task, and thus was a prospective template in relation to the first search task. The meaning of the two outline cues was counterbalanced across subjects. We will refer to the target for the first search task as the *first template*, while the target representation for the second search task served as what we will refer to as the *second template*. The other two colors had a full outline and were presented merely for sensory balancing purposes; subjects were told they could completely ignore these items. The memory display was followed by a delay period of 1400 ms, during which subjects focused on a fixation cross. This was followed by two consecutive search tasks, which were presented until response and separated by a second delay period of 1800 ms. Subjects received a 50 ms auditory cue at the onset of each display (memory, search 1 and search 2). Subjects were required to find the color memorized for the respective search task and indicate the direction of the arrowhead plotted inside the target by clicking a button (placed on both armrests) that corresponds to the direction of the arrowhead (i.e., left hand button for leftwards pointing arrowhead and vice versa). The second response was immediately followed by the fixation cross of the next trial. If subjects failed to respond within 5 s, they were shown the message: “Too slow! Please respond faster”. Subjects were instructed to focus on the central fixation cross during the inter-trial interval (ITI), the memory display and both delay periods.

The first experimental manipulation was the location at which the first and second templates were presented in the memory display (Table 1 and Fig. 1B). In the First Template Lateralized condition the first template was presented left or right from central fixation while the second template was presented on the central meridian, above or below fixation. In the Second Template Lateralized condition the second template was presented lateralized while the first template was presented on the meridian. In the Both Lateralized condition both the first and the second template were presented lateralized, on opposite sides of central fixation. With this design we manipulated the task relevance that the lateralized memory

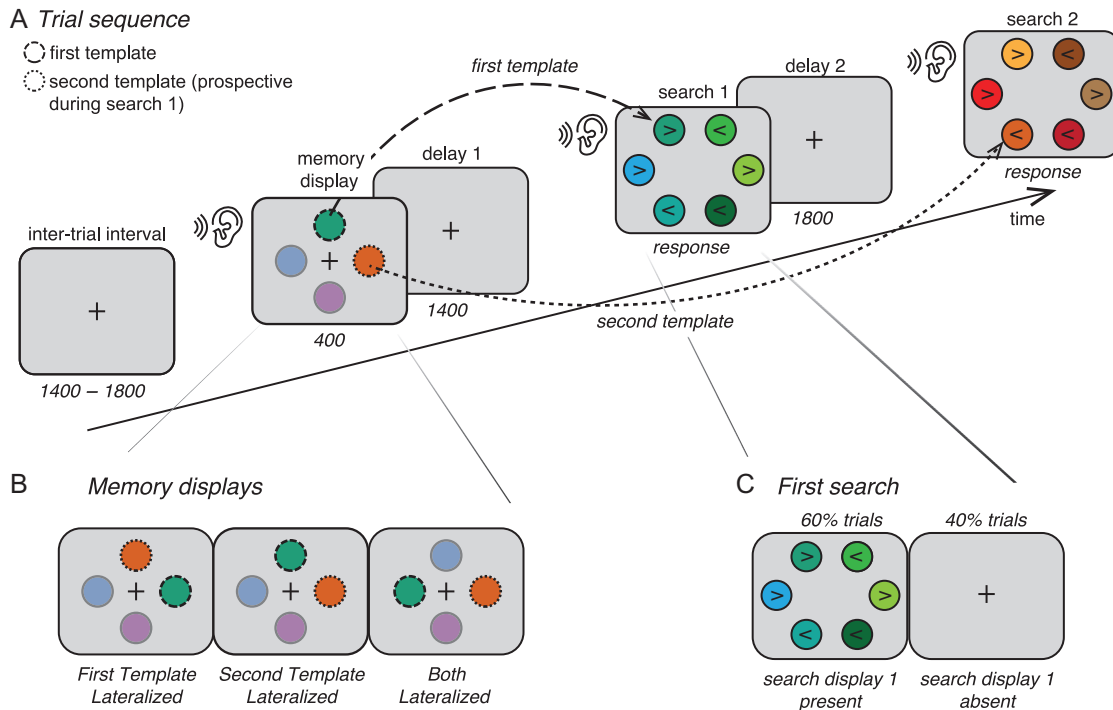


**Figure 1.** Task design. (A) Trial sequence. Observers were given two targets to remember for two consecutive search tasks; one for the first search task (*first template*; dashed outline), and one for the second search task (*second template*; dotted outline). The onset of every stimulus display was accompanied by an auditory cue (sound/ear symbol). (B) In the *First Template Lateralized* condition, the first template was presented lateralized (left or right), while the second template was presented on the meridian (up or down). In the *Second Template Lateralized* condition this was the other way around. In the *Both Lateralized* condition, both memory items were presented lateralized, at opposite sides (left/right positions were counterbalances across trials in all conditions). (C) In 60% of trials subjects first conducted the first search, followed by the second. In 40% of trials, the first delay period was not followed by the first search display, and the screen remained blank (with a fixation cross) as the second delay period started. However, the auditory cue still sounded, thus indicating that the first search could be abandoned and that observers should switch to the second search task, and look for the second target instead. For illustrative reasons, object sizes and colors differ from the real experiment and the opacity for the irrelevant colors in the memory displays is set at 50%.

**Table 1.** Condition properties

Condition	Included in cue-locked analyses delay 1	Included in switch-locked analyses delay 2	Total trial amount (per block)	Location first template	Location second template
<b>First search present</b>					
First Template Lateralized	Yes	No	180 (6)	Left or right	Top or bottom
Second Template Lateralized	Yes	No	180 (6)	Top or bottom	Left or right
Both Lateralized	Yes	No	180 (6)	Left or right	Left or right
<b>First search absent</b>					
First Template Lateralized	Yes	Yes	120 (4)	Left or right	Top or bottom
Second Template Lateralized	Yes	Yes	120 (4)	Top or bottom	Left or right
Both Lateralized	Yes	Yes	120 (4)	Left or right	Left or right

item acquired prior to the search task itself (current or prospective), which enabled us to directly relate lateralized EEG patterns to either a currently relevant or prospectively relevant item in VWM. The second manipulation was the unexpected absence of the first search task, which occurred in 40% of trials (Fig. 1C). Importantly, the auditory cue that indicated the onset of the first search task was still present, but was instead directly followed by the second delay period, leading up to the second search task. The combination of the auditory cue and the absence of a change in visual stimulation on the screen

(i.e., no first search display), thus informed subjects that they could internally drop the first template, in favor of now prioritizing the second template. Our main analyses, aimed at revealing EEG signatures of endogenous priority switches within VWM, thus focused on these 40% of trials in which the first search display was absent, and which were thus free from signals reflecting the visual input from the first search display.

Subjects performed the EEG experiment in two sessions on separate days, to minimize mental fatigue. Each session started with a practice block followed by 15 real blocks. Each block

contained the same randomly ordered composition of 30 trials: 10 per condition (First Template Lateralized, Second Template Lateralized and Both Lateralized), and for each condition 6 with and 4 without first search task (Table 1). During the practice block subjects received feedback after each trial, but in the real experiment only during the short breaks between blocks.

## Stimuli

Subjects were comfortably seated in a sound attenuated and electrically shielded room. The chair and screen were placed at individual height and two response buttons on the armrests made sure the arms were in a relaxed and comfortable position. The viewing distance was 75 cm from a 22-inch video monitor (Samsung Syncmaster 2233, 1680×1050 pixels at 120 Hz). The stimuli were created using OpenSesame version 2.9.0 (Mathôt et al. 2012, RRID:SCR\_002849), a Python based graphical experiment builder.

The background color was gray (81 Cd/m<sup>2</sup>). The fixation cross was a black plus sign (0.6° of line length). In the memory display, the 4 colored circles were presented 1.5° left, right, above, and below of the fixation cross. The circles had a radius of 0.6° with a black outline of 0.09° that was dashed, dotted or full. The visual search display contained 6 colored circles, presented equidistantly on an imaginary circle with a radius of 4°. These parameter values fall well within a range of commonly used values that have been shown to produce lateralized EEG patterns such as the CDA and lateralized alpha suppression (Woodman and Arita 2011; Gunseli et al. 2014; de Vries et al. 2017). The arrowhead pointed either left or right (< or >) and was drawn in the center of each circle (always 3 left- and 3 right-pointing arrows, randomly divided across all 6 items). The auditory cue was generated by OpenSesame's built-in synthesizer, consisted of a 50 ms 660 Hz sine wave and was presented by a HK195 speaker.

Stimuli colors were strictly controlled to discourage verbalization and encourage VWM use. In total there were 12 colors created in DKL color space (Derrington et al. 1984) that were equidistant in hue (from 12 to 324 degrees in steps of 24, skipping 108 and 156 because they were subjectively too similar) while being constant in the other two dimensions, i.e., contrast = 1 and luminance = 0 (i.e., isoluminant). This created an imaginary circle of 12 discrete colors (41.2 ± 4 Cd/m<sup>2</sup>, slight deviation from isoluminance due to not perfectly calibrated screen), with those opposite from each other being least similar in hue and those next to each other being most similar in hue. The target color for the first search display (first template) was randomly chosen, after which the second target color (second template) was chosen as the opposite (i.e., least similar) color on the color circle. While this introduces some regularity into the design that could potentially be used as a strategy (i.e., after learning the regularity participants could decide to only memorize the first template and retrieve the second template from long-term memory (LTM), after first having encoded these color-space pairs in LTM), we reasoned the easier strategy would be to keep both colors and their status temporarily in VWM, on each consecutive trial (and which was confirmed by the results). The other two colors in the memory display (to be ignored) were two colors in between the currently and prospectively relevant color on the color circle, but at least 2 steps away from either. The other 5 colors in the search display were randomly chosen from 8 colors surrounding the memorized color on the color circle, thus making them relatively similar in hue to the memorized color. While this selection procedure encouraged visual memorization of the stimuli, we cannot

completely exclude that some degree of verbalization took place. However, verbalization would most likely diminish rather than inflate the lateralized EEG signals of interest here, making it unlikely to be a confounding factor.

## Data Recording and Preprocessing

EEG data were acquired at 512 Hz using a 64-electrode cap (BioSemi, Amsterdam, The Netherlands; ActiveTwo system, 10–20 placement; [biosemi.com](http://biosemi.com)), and from both earlobes (used as reference). Vertical and horizontal EOG were recorded from electrodes located 2 cm above and below the right eye, and from electrodes 1 cm lateral to the external canthi, respectively. The HEOG was used to detect horizontal eye movement artifacts. Offline analyses were performed in Matlab (2014, The Mathworks, RRID:SCR\_001622). All preprocessing steps were performed on the EEG data sets of the 2 measurement sessions separately.

EEG data were re-referenced to the average of left and right earlobes and filtered using a 0.1 Hz high-pass filter (least-squares FIR). Continuous EEG was epoched from -2.5 to 7 s surrounding memory display onset. Epochs were baseline-normalized using the whole epoch as baseline for the improvement of independent component analysis (ICA (Groppe et al. 2009)). Before trial rejection, data were visually inspected and one ( $n = 6$ ), two ( $n = 2$ ) or three ( $n = 1$ ) malfunctioning electrodes were temporarily removed. To detect epochs contaminated by EMG artifacts, we used an adapted version of an automatic trial-rejection procedure as implemented in the Fieldtrip toolbox (Oostenveld et al. 2011, RRID:SCR\_004849). We used a 110–140 Hz band-pass filter to specifically capture muscle activity, and allowed for variable z-score cut-offs per subject based on within-subject variance of z-scores. This resulted in an average cut-off of  $18.9 \pm 4.7$ , which in turn resulted in a rejection of 4.9% (min–max across subjects: 0.2–11.1%) of all trials. Next, we performed ICA as implemented in the EEGLAB toolbox (Delorme and Makeig 2004, RRID:SCR\_007292) on clean trials and electrodes only. We visually inspected the VEOG signal together with the ICA components and removed those that captured eye-blinks, eye movements, or other clearly not brain-driven artifacts (1.65 components on average), after which we interpolated the malfunctioning electrodes identified earlier using spherical spline interpolation as implemented in EEGLAB's `eeg_interp.m` function. Finally, we detected trials with large horizontal eye-movements using the `pop_artstep.m` function in ERPLAB (Lopez-Calderon and Luck 2014, RRID:SCR\_009574), applied on the 1 Hz high-pass filtered HEOG signal, with a window length of 400 ms, a step size of 10 ms, during a time window of -50 to 900 ms surrounding memory display onset, and with individual thresholds of  $24.7 \pm 12$ . Using these settings we detected sudden sharp jumps in the HEOG surrounding the lateralized memory display onset and during start of the delay period. During this interval it was most important to keep fixation, as an eye movement towards, and subsequent fixation on, a laterally presented memory item would dampen our lateralized EEG measures (i.e., when the eyes fixate on the memory item, contra- and ipsilateral effectively become undefined). This procedure resulted in a rejection of 5.7% (min–max across subjects: 0.4–14.7%) of all trials. Additionally, we analyzed the presence of systematic horizontal eye movements towards or away from the memorized template locations, around the time window of the auditory switch cue, and how these might influence our EEG signals of interest (see online Supplementary Material).



After trial rejection based on the EEG signals, we rejected trials with incorrect responses in either one of the two search tasks (19%, min–max across subjects: 9–28%). We also applied a two-step reaction time (RT) trimming: trials with a response faster than 300 ms and slower than 5000 ms were rejected, after which trials with a response of 3 standard deviations above or below the condition- and search-specific mean were excluded. This led to a rejection of 1.8% of all trials (min–max across subjects: 0.4–3.3%). After all trial rejection steps (RT, noise, incorrect response and horizontal eye movements) an average of 71% of all trials was left (mean/min–max % across subjects: First Template Lateralized: 72/59–84; Second Template Lateralized: 71/62–80 Both Lateralized: 70/63–78). These correct and clean trials were divided according to condition (Table 1) and side of the lateralized memory item (left or right) during memory display. For the Both Lateralized condition, contra- and ipsilateral were defined relative to the first template. Whereas all trials were used for analyses of the first (cue-locked) delay period, only trials without a first search task (40%) were used for the analyses of the second (switch-locked) delay period (Table 1). After these preprocessing steps, we concatenated the EEG data files of the 2 sessions for each subject.

## Time–Frequency Decomposition

### Laplacian

First we estimated the surface Laplacian (Perrin et al. 1989), a spatial high-pass filter that accentuates local effects while filtering out distant effects due to volume conduction, consequently sharpening the EEG topography (Cohen 2014; Kayser and Tenke 2015). We used a 10th-order Legendre polynomial and a lambda of  $10^{-5}$  to estimate the surface Laplacian.

### Morlet Wavelet Convolution

Epoched EEG time series were decomposed into their time–frequency representations by means of Morlet wavelet convolution for frequencies ranging from 1 to 40 Hz in 25 logarithmically spaced steps, using custom-writing Matlab scripts. A Gaussian ( $e^{-t^2/2s^2}$ , where  $s$  is the width of the Gaussian) was multiplied with 25 sine waves ( $e^{i2\pi ft}$  where  $i$  is the complex operator,  $f$  is frequency, and  $t$  is time) to create the complex Morlet wavelets. The width was set as  $s = \delta/(2\pi f)$ , where  $\delta$  represents the number of cycles of each wavelet, logarithmically spaced between 3 and 12 to have a good trade-off between temporal and frequency precision. Frequency-domain convolution was applied, i.e., the Fast Fourier Transform (FFT) was applied to both the EEG data and the Morlet wavelets, after which these were multiplied. The inverse FFT was applied to the result to convert the signal back to the time domain. Power at each time point and each frequency was defined as the squared magnitude of the complex signal resulting from the convolution, i.e.,  $[\text{real}(Z_t)^2 + \text{imag}(Z_t)^2]$ . After averaging power over trials per condition, decibel normalization was applied per frequency and per channel  $[\text{dB Power}_{tf} = 10 \cdot \log_{10}(\text{Power}_{tf}/\text{Baseline Power}_{tf})]$ , with condition-average power 500 to 200 ms before memory display-onset as baseline.

### Connectivity Analyses: Amplitude–amplitude and Phase–Amplitude Coupling

To test our hypothesis of a functional role for frontal low frequency power in the top-down control of the priority switch within VWM, we estimated functional connectivity between lateralized posterior alpha power and frontal delta power and phase by means of amplitude–amplitude and phase–amplitude co-modulations, specific manifestations of cross-frequency

coupling known to support large-scale cortical network interactions (Siegel et al. 2012; Helfrich and Knight 2016). First, we determined the time–frequency cluster that showed a significant ( $P < 0.001$ ) condition-average frontal delta power increase following the auditory switch cue (Fig. 5A), using group-level cluster-based permutation testing (see subsection Statistics). In our initial connectivity analysis, we specifically tested for a relationship between the frontal delta power cluster (Fig. 5A) and lateralized posterior alpha power (Fig. 4B). That is, we averaged for each subject, condition, and single trial the power within the above-mentioned frontal delta cluster and correlated these raw power values across trials with the raw alpha power values in posterior electrodes (similar to e.g., Mazaheri et al. 2009). Note that we kept the a priori selected posterior electrodes for alpha power fixed, which thus served as seeds, and correlated these with delta power in the 9 a priori selected frontal electrodes (Fig. 5A; see subsection Electrode, Frequency and Time Window Selection). This procedure resulted in a within-subject correlation time series at each of the 9 frontal electrodes, linking early frontal delta to subsequent lateralized posterior alpha power at the single-trial level. We used Spearman's rank correlation and coefficients were Fisher z-transformed to obtain normally distributed values before applying statistical analyses (Silver and Dunlap 1987).

On the one hand, the above approach allows for a predictive inference: early delta power may correlate with lateralized alpha power later in time. However, this analysis does not speak to the underlying neurophysiological mechanism of frontal-posterior communication. To gain further insight into the delta-alpha coupling, we performed an exploratory phase–amplitude coupling analysis. Indeed, the coupling of low frequency phase to high frequency power or to neuronal spiking has been proposed as a physiologically plausible mechanism for information transfer within and between regions (Buzsáki et al., 2004; Jensen and Colgin 2007; Canolty and Knight 2010). In brief, we estimated for each trial whether the difference between the instantaneous phase angles of frontal delta oscillations and the power envelope of posterior alpha oscillations was consistent over time within that trial (see online Supplementary Material for details).

### Brain–Behavior Relationship

In order to investigate whether frontal delta oscillations supported behavior (Helfrich et al. 2017), we also correlated for each subject, electrode and time point, delta power time series averaged over 2–6 Hz (see subsection Electrode, Frequency and Time Window Selection) with the reaction time on the second search task across trials, using Spearman's rank correlation. Correlation coefficients were Fisher z-transformed.

### Electrode, Frequency and Time Window Selection

All selection procedures were performed on condition-average data and were thus orthogonal to and unbiased by any observed condition difference. Statistical comparisons were done only after these selection procedures (see subsection Statistics). The first step was to select channels that would show lateralized posterior alpha suppression. Based on previous results from our lab (de Vries et al. 2017; van Driel et al. 2017), we a priori selected O1/2, PO3/4, and PO7/8. Furthermore, we visually inspected the topographical map of the left- versus right-cue contrast in the time–frequency window that showed a significant contra- versus ipsilateral contrast in the condition-average (Fig. 3A). The result of this procedure

supported our a priori electrode selection. We determined the significant condition-average time-frequency cluster during the first delay (see black outline in the time-frequency plot in Fig. 3A) through group-level cluster-based permutation testing on the contra- versus ipsilateral contrast (see subsection Statistics). Similar to our electrode selection, the frequency range for our posterior alpha lateralization analysis (8–14 Hz) in the second delay was also selected a priori based on our previous findings (de Vries et al. 2017; van Driel et al. 2017), and further supported by the (although at some points slightly wider) significant time-frequency cluster as found in the current study (Fig. 3A). Importantly, the a priori selected posterior electrodes (O1/2, PO3/4 and PO7/8) and frequency range (8–14 Hz) were kept fixed for all further analyses involving posterior alpha lateralization (Fig. 4B and 5B).

For our cross-frequency coupling analyses, we initially selected a large spatial area consisting of 9 mid-frontal electrodes (AFz/3/4, Fz/1/2, and FCz/1/2, see left column in Fig. 5A). Next, through group-level cluster-based permutation testing (see subsection Statistics) we determined the condition-average time-frequency cluster showing a significant increase in frontal delta power relative to baseline (see black outline in the right column in Fig. 5A). This time-frequency cluster was used in the analysis of computing Spearman correlation between delta power and lateralized posterior alpha power (Fig. 5B), and the frequency range in this cluster (2–6 Hz) was used in the analysis of correlating delta power with reaction time (Fig. 5C). Time-frequency analysis inherently involves a trade-off between spectral and temporal precision, resulting in a relatively low temporal precision for low-frequency wavelets. In the current task design where displays follow each other rapidly, this causes inaccurate estimates of the timing of low-frequency activity. For example, in the estimation of 1 Hz power directly following the auditory switch cue, power modulations evoked by the first and second search tasks leak into the signal. For this reason we excluded frequencies below 2 Hz for all analyses involving frontal delta power. The time interval selected for the topographies in the left column of Figure 5B and C (475–900 ms) is based on the condition-contrast for posterior alpha lateralization (see Fig. 4B) and is merely selected as an example time window for illustrative purposes. Similarly, the electrodes selected for the time series in the right column (indicated by white disks in topographies in left column) also reflect example electrodes selected for illustrative purposes. Importantly, for the correlation analysis (Fig. 5B) the posterior electrodes for the lateralized alpha power time series described above were kept fixed (and thus served as seed electrodes). Accordingly, this procedure resulted in lateralized correlation time series (Fig. 5B) at the 9 a priori selected frontal electrodes, which were all included in a time-by-channel cluster-based permutation test (see subsection Statistics). For the correlation between delta power and reaction time (Fig. 5B), we did not a priori select any electrodes, and so this correlation value was calculated at all 64 electrodes, which were all included in the time-by-channel cluster-based permutation test.

## Statistics

For our behavioral data, we used JASP (Version 0.7.1.12, RRID: SCR\_015 823), a GUI software package for performing Bayesian statistics (Love et al. 2015). Bayesian hypothesis testing directly evaluates the strength of evidence for one hypothesis (H1) over the alternative (null) hypothesis (H0), and this evidence is quantified by the Bayes Factor (BF) (Wagenmakers et al. 2017). A BF of 10 for example, indicates that H1 is 10 times more likely than H0,

given the observed data. In contrast, a BF of 0.1 indicates that H0 is 10 times more likely than H1. Thus, in contrast to traditional statistics, this method allows for a direct quantification of the evidence in favor of the null hypothesis (Rouder et al. 2009). A BF of 1 to 3 reflects anecdotal evidence, 3 to 10 moderate evidence, 10 to 30 strong evidence, 30 to 100 very strong evidence, and 100 or higher extremely strong evidence in support of H1 (Wagenmakers et al. 2017). In all our Bayesian analyses, we used the default model parameters and prior distributions as set by JASP. RT and accuracy for first and second search task were entered into a Bayesian equivalent of a repeated measures ANOVA, with the within-subject factor Condition (First Template Lateralized, Second Template Lateralized and Both Lateralized). Furthermore, using a Bayesian equivalent of a paired-sample t-test, we tested whether there was a difference in RT and accuracy between the first and second search task, and between the first search task absent and first search task present trials.

Statistical testing of EEG time or time-frequency signals involves many comparisons (each time-, frequency-, and/or electrode-point). Thus, we performed group-level non-parametric permutation testing with cluster-based correction for multiple comparisons, which effectively controls for the auto-correlation over time, frequency and space in the EEG signals (Maris and Oostenveld 2007; Maris 2012). In a first step, we tested the time-frequency maps of the condition-average power at our a priori selected posterior electrodes for a difference between electrodes contra- and ipsilateral to the lateralized memory item. A paired-sample t-test was performed on each time-frequency point and a threshold was set at a certain P-value (see section Results for the specific threshold per analysis, set at 0.05 or lower), resulting in clusters of significant time-frequency points. Next, in each of 2000 iterations, the contra- and ipsilateral labels were randomly shuffled across subjects and the same paired-sample t-test was performed on the contra- versus ipsilateral difference in these “surrogate” data at each time-frequency point. The sum of t-values within the largest cluster of significant time-frequency points in each iteration was used to create a distribution of summed cluster t-values under the null-hypothesis of no contra- versus ipsilateral difference. The percentile of the null-hypothesis distribution corresponding to the same P-value as for the t-test (e.g., the 99th percentile for  $P < 0.01$ ) was used as threshold for the summed cluster t-values of the significant clusters in the observed data. Thus only significant clusters that are larger than what can be expected by chance, survive this procedure (e.g., see black outline, Fig. 3A). This permutation test was unbiased by potential condition differences, since it was performed on the condition-average data.

### First Delay Activity Time-locked to Memory Cue

For the analysis of the first delay period, we directly tested whether we could replicate our previous findings (de Vries et al. 2017), i.e., whether lateralized posterior alpha suppression is stronger for current than for prospective templates during the first delay period. Following a similar procedure (de Vries et al. 2017), we averaged the lateralized posterior alpha power per condition over the time-frequency points within the significant condition-average cluster (see Fig. 3B). Next we performed 2 Bayesian equivalents of paired-sample t-tests using JASP. In the first test we evaluated the difference between the First Template Lateralized and the Second Template Lateralized conditions. Because in the Both Lateralized condition the first and second templates were always presented opposite from each other, contralateral to the first template was simultaneously

ipsilateral to the second template, and vice versa. Therefore, in the second statistical test we evaluated the difference between electrodes contralateral to the first template and electrodes contralateral to the second template (which inherently were ipsilateral to the first template). This test allowed us to directly compare relative alpha suppression for the first and second template when they are competing in terms of lateralized EEG measures.

### Second delay activity time-locked to auditory switch cue

For the analysis of lateralized posterior alpha power during the second delay period after the auditory switch cue, we first averaged over the alpha frequency range (8–14 Hz) and subtracted ipsi- from contralateral electrodes. Next, we performed the same non-parametric permutation test as described above with the significant threshold set at  $P < 0.05$ , but now on the condition-contrasts, and at all time points instead of time-frequency points.

For the connectivity between lateralized posterior alpha power and frontal low-frequency power, we did not have hypotheses about the exact frontal electrode, or the exact frequency range. First, a significant condition-average local frontal delta power cluster (Fig. 5A) was derived using the same permutation procedure as described above with the significant threshold set at  $P < 0.001$ , but now to test for power significantly different from baseline. Next, we averaged over the delta frequency range based on this cluster, but excluding frequencies below 2 Hz (see subsection Electrode, Frequency and Time Window Selection). To test for condition-differences in the correlation between the frontal delta power cluster and lateralized posterior alpha power, we performed a permutation test on the condition difference with the significant threshold set at  $P < 0.05$ , over the correlation values at the 9 a priori selected frontal electrodes and all time points (Fig. 5A). Similarly, to test for a significant condition-average correlation between frontal delta and RT2, we performed a permutation test with the significant threshold set at  $P < 0.05$ , but now including all time-points and all 64 electrodes for the delta time series. We used Fieldtrip's `ft_prepare_neighbours.m` function with the method parameter set to "template" to define which electrodes are neighbors, and we used the `ft_timelockstatistics.m` function with the method parameter set to "montecarlo" to run the permutation test for all time-electrode points (Maris and Oostenveld 2007; Oostenveld et al. 2011). In the latter function, the minimum number of neighboring significant electrodes to define whether electrodes were part of the same significant cluster was set to 1.

## Results

### Behavioral Analyses: Current and Prospective Templates are Encoded and Maintained Equally Well

We analyzed the behavioral data with Bayesian statistics (see Methods) as provided by the open source JASP toolbox (Love et al. 2015), and report the Bayes Factor (BF) for support of the alternative over the null hypothesis (Wagenmakers et al. 2017). In general, participants performed accurately (mean/min-max % correct: first search task: 91/84-95; second search task [first search task present]: 82/70-93; second search task [first search task absent]: 90/81-97; Fig. 2, upper panel). However, performance on the second search task declined if it was preceded by a first search task ( $BF = 1.2 \cdot 10^4$ ). Importantly though, second search task performance on trials in which the first search task was omitted was comparable to first search task performance

( $BF = 0.30$ ; a BF lower than 0.33 indicates moderate evidence for no condition difference). Reaction times showed a similar pattern (Fig. 2, lower panel). That is, subjects responded slower in the second search task if it was preceded by a first search task ( $BF = 15.9$ ), whereas second search task response times for trials in which the first search task was omitted were comparable with average first search task response times ( $BF = 0.30$ ). As expected, there were no differences for the 3 lateralization conditions ( $BF < 0.30$  for all search tasks). Together, this pattern of results indicates that observers remembered the two search targets equally well, but that second search performance suffered as a consequence of interference from the first search task. Thus, experimentally manipulating the priority states of the VWM representations in itself did not affect the quality of the memory per se.

Although the spatial location of the memory items was task-irrelevant, our expectations in terms of alpha lateralization are based on the assumption that observers will still use the spatial information to both encode and retrieve the information (whether implicitly or explicitly). To explore whether this would also be reflected in the behavioral data, we tested for a spatial congruency effect between the memorized cues and the eventual target in the first search display. Interestingly, participants responded faster (mean  $\pm$  SEM:  $804 \pm 20$  ms vs.  $828 \pm 24$  ms,  $BF = 8.1$ ) and more accurately ( $92.8 \pm 0.8\%$  vs.  $90.6 \pm 1\%$ ,  $BF = 3.8$ ) when the first target was presented in the same hemifield as where the first template was presented. In contrast, participants responded slower ( $822 \pm 21$  ms vs.  $805 \pm 21$  ms,  $BF = 6.9$ ) and slightly less accurate (i.e., numerically but not statistically;  $90.5 \pm 0.8\%$  vs.  $91.4 \pm 0.8\%$ ,  $BF = 0.7$ ) when the first target was presented in the same hemifield as where the second template was presented. Albeit speculative, this

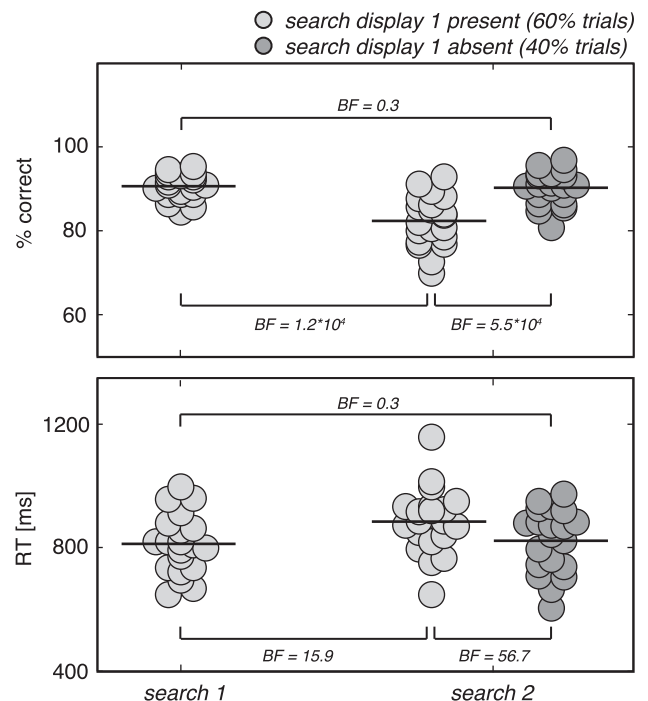


Figure 2. Behavioral results. Dots represent single subject behavioral data (percentage correct and reaction time in upper and lower panel, respectively), averaged over the 3 possible memory displays (see Fig. 1B). Horizontal line segments represent the mean across subjects. BF = Bayes factor for H1 over H0, with H1 and H0 being a difference or no difference between conditions, respectively.



suggests that sensory regions that encoded the first search template were enhanced, while those that processed the second search template were suppressed during the first search.

### Priority in VWM Reflected in Lateralized Posterior Alpha Suppression

EEG was decomposed into its spectrotemporal representation of frequency-specific power and phase, using Morlet wavelet convolution (see Methods). The posterior electrodes for the alpha power analyses (O1/2, PO3/4, PO7/8) were selected a priori based on previous findings (de Vries et al. 2017; van Driel et al. 2017), and were kept fixed for all further analyses. Power in the alpha band (8–14 Hz) was more suppressed (relative to a pre-stimulus baseline) for contralateral compared with ipsilateral electrodes during the first delay period (425–1050 ms relative to memory display onset,  $P < 0.01$  cluster-corrected,  $BF = 1.3 \times 10^4$ ; Fig. 3A). Lateralization of alpha suppression during working memory encoding and maintenance is a robust finding, and has been interpreted as a “functional inhibition” mechanism for the suppression of irrelevant vis-à-vis the selection of relevant sensory information (Fukuda et al. 2015; Myers et al. 2015b; van Driel et al. 2017). Similar to our previous study (de Vries et al. 2017), we then averaged per condition over the time–frequency points that were significant in the condition-average (see black outline in Fig. 3A), in order to test for condition differences. Importantly here, during the first delay period leading up to the first search task, lateralized alpha suppression was stronger for the first than for the second template (Fig. 3B). This was true when only one item was presented lateralized (First Template Lateralized > Second Template Lateralized,  $BF = 26.4$ ), as well as when the first and second templates were presented opposite from each other (Both Lateralized: contralateral to first template > contralateral to second template,  $BF = 83.0$ ). Thus, we found that the lateralization of alpha suppression was sensitive to the priority status of VWM representations during the first delay period in a two-consecutive search-task experiment, which is a replication of our earlier work (de Vries et al. 2017).

### Neural Signature of Priority Switches Between VWM Representations

Next, we tested whether posterior alpha lateralization was sensitive to switching from one template to the next during the second delay period that led up to the second search task. As stated above, for this we only used those trials in which the first search task was omitted, and the second delay was time-locked to the auditory signal. As our hypothesized frequency-band of interest was based on our previous findings (de Vries et al. 2017; van Driel et al. 2017) we a priori averaged over frequencies within the alpha range of 8–14 Hz. Furthermore, because the statistical tests performed on the rest of our metrics all involved cluster-based permutation testing over multiple dimensions (channel, time and/or frequency; see subsection Statistics) we did not perform additional Bayesian statistics on these metrics.

This analysis revealed 3 important findings. First, we found that the auditory switch cue triggered a re-emergence of lateralized alpha suppression associated with the second template (Fig. 4B, orange line; Second Template Lateralized). Importantly, after this cue the second template became the new currently relevant template. Second, the fact that the first template was now no longer task-relevant resulted in relative alpha

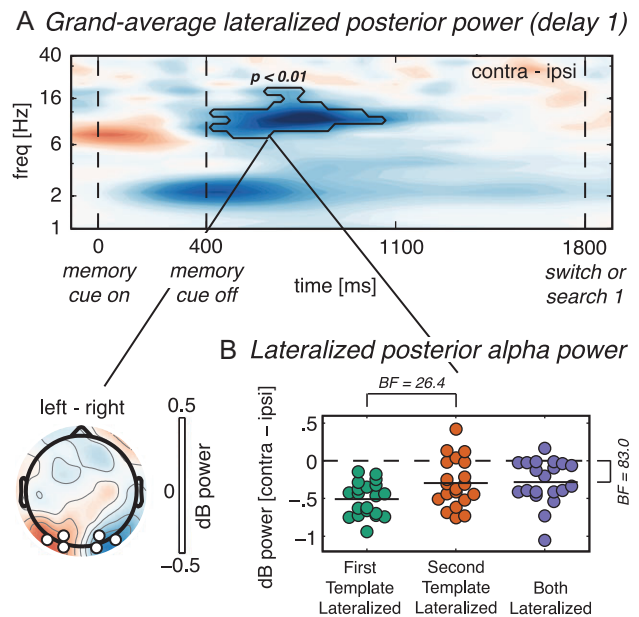


**Figure 3.** Priority in VWM is reflected in lateralized posterior alpha suppression. (A) Time–frequency plot of lateralized (contralateral minus ipsilateral) power at the average of O1/2, PO3/4 and PO7/8 during the memory display and the first delay period, averaged across all conditions. Black outline indicates a significant difference between contra- and ipsilateral power in the condition average at  $P < 0.01$ , cluster corrected. The topography indicates the condition-average scalp distribution of alpha power in the significant time–frequency cluster, on trials with the memory item on the right subtracted from trials with the memory item on the left; black-bordered white disks mark the pre-selected electrodes. (B) Dots represent single subject data of lateralized power averaged over the time–frequency cluster highlighted in (a), with each condition indicated by a different color. Horizontal lines in the dot clouds represent the mean across subjects.  $BF = 26.4$  indicates a difference between First Template Lateralized and Second Template Lateralized, whereas the  $BF$  of 83.0 indicates that Both Lateralized is significantly different from baseline.

enhancement for trials in which the first template had been presented lateralized (Fig. 4B, green line; First Template Lateralized). This contrast was reflected in a significant difference between the First Template Lateralized and Second Template conditions from 475 to 900 ms following the switch cue ( $P < 0.05$ , cluster-corrected). Third, before the above effects, right around the expected time of the first search task, lateralized alpha power was enhanced for the second template, but not for the first template (–100 to 300 ms;  $P < 0.05$ , cluster-corrected). This is consistent with participants anticipating the first search display and thus temporarily de-prioritizing the second template in order for it not to interfere with the first search task. The time–frequency plot of the contrast between the First Template Lateralized and Second Template Lateralized conditions (Fig. 4A) confirmed that the peak of the switch fell within the a priori selected frequency band (8–14 Hz).

Finally, the Both Lateralized condition (Fig. 4B, purple line) corroborated the above pattern. In this condition, the first and second templates were both presented lateralized, at opposite sides (see Fig. 1B). Here we defined contra- and ipsilateral relative to the first template, and thus electrodes located contralateral to the first template consequently were located ipsilateral to the second template, and vice versa. In this condition then, alpha lateralization reflects a combination of prioritizing one



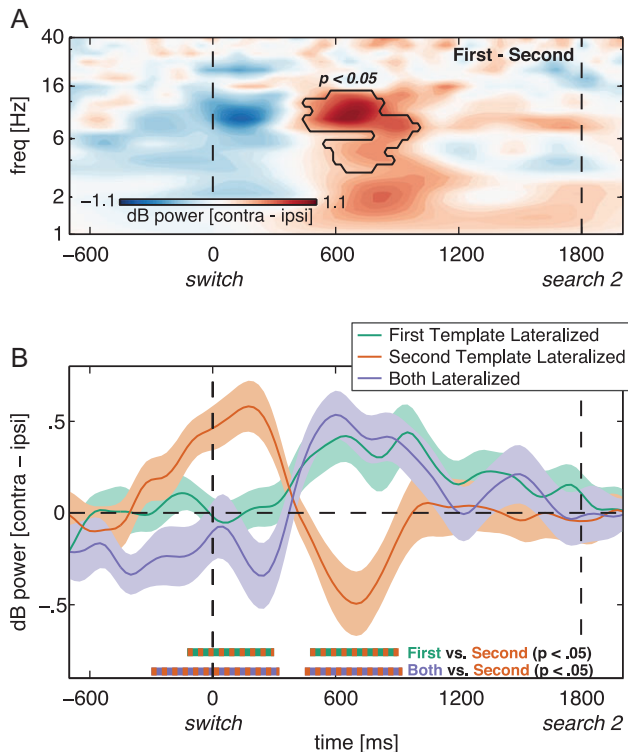


**Figure 4.** Neural signature of priority switches between VWM representations. (A) Time–frequency plot of lateralized (contralateral minus ipsilateral) power at the average of O1/2, PO3/4 and PO7/8 during the second delay period (time-locked to the auditory switch cue), for the First Template Lateralized versus Second Template Lateralized condition-contrast. Black outline indicates a significant difference in lateralized power between First Template Lateralized and Second Template Lateralized at  $P < 0.05$ , cluster corrected. (B) Time series of lateralized alpha (8–14 Hz) power at the above-mentioned electrodes for First Template (green), Second Template (orange) and Both (purple) Lateralized memory display conditions. The thick lines and shaded areas denote subject mean and standard error of the mean, respectively. Standard errors are calculated for normalized data, i.e., corrected for between-subject variability (Cousineau 2005; Morey 2008). Double-colored thick lines on the x-axis indicate time points with a significant difference between the respective conditions after cluster correction at  $P < 0.05$ . Only data from the trials where the first search display was absent (40% of all trials) are depicted in this figure.

and de-prioritizing the other item, making it impossible to distinguish the two effects. Nevertheless, we observed two interesting patterns that fit well with the effects observed in the First Template Lateralized and Second Template Lateralized conditions. First, the prioritization of the second, and the de-prioritization of the first template, resulted in alpha enhancement contralateral to the first template and thus simultaneously, alpha suppression contralateral to the second template (450–925 ms;  $P < 0.05$ , cluster-corrected). This pattern corresponds to the effects observed in the First Template Lateralized and Second Template Lateralized condition, respectively. Second, around the expected time of the first search task (i.e., around the time of the auditory switch cue), alpha was suppressed contralateral to the first template and thus simultaneously, alpha was enhanced contralateral to the second template (–300 to 325 ms;  $P < 0.05$ , cluster-corrected). This latter effect is what we also observed in the Second Template Lateralized condition. We would like to mention that in those 60% of trials where the first search display was present (Fig. 1C and Table 1), there were no significant effects of alpha lateralization in the second delay period (data not shown). This is

consistent with our previous study (de Vries et al. 2017), and is likely due to the fact that this time interval directly followed the first search task and first response, which possibly contaminated subsequent EEG signals.

In sum, our results show that prioritizing and de-prioritizing VWM representations during maintenance are reflected in both alpha suppression for to-be-attended items and alpha enhancement for to-be-dropped or temporarily unattended items, respectively, over posterior regions that process those representations.

### Connectivity Between Frontal and Posterior Regions During Priority Switch in VWM

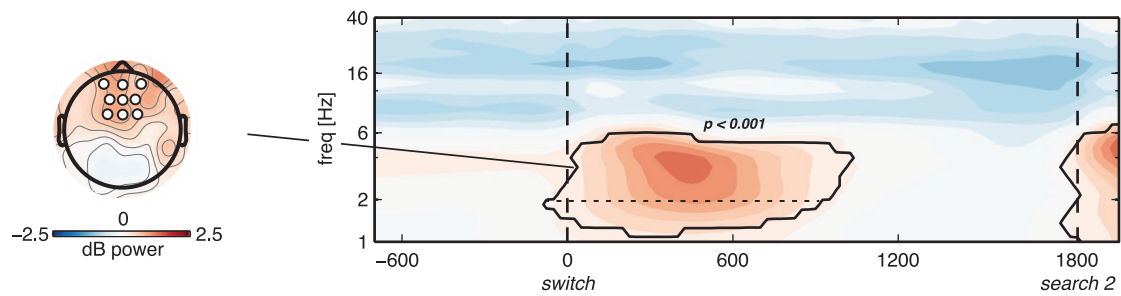
Next, we investigated the involvement of frontal low-frequency oscillations in the top-down control of the priority switch. Across all conditions, power in the delta/low-theta frequency band (1–6 Hz) increased relative to baseline shortly after the cue to switch (–75 to 1025 ms,  $P < 0.001$ , cluster-corrected; Fig. 5A). Such an increase in low-frequency power in frontal regions has been a consistent finding in various VWM tasks that require top-down control (Sauseng et al. 2010; Johnson et al. 2017), and thus does not reflect its specific involvement in priority switches per se.

Through both amplitude–amplitude correlation and phase–amplitude coupling analysis, which reflect transient large-scale functional connectivity dynamics (Siegel et al. 2012), we specifically studied whether and how frontal delta power and phase predicted lateralized posterior alpha power, and how this would support the switch in lateralization. Indeed, condition-average alpha lateralization mainly correlated with delta power in frontal electrodes (Fig. 5B, topoplot). Importantly, the lateralized correlation measure revealed a condition contrast between First Template Lateralized and Second Template Lateralized in the same direction and time interval as the contrast between the same conditions when assessing local posterior alpha lateralization alone (compare Fig. 4B with Fig. 5B). Specifically, the cue to switch was directly followed by an increase in frontal delta power (Fig. 5A). In trials in which the second template was presented lateralized (Fig. 5B; orange line), an increase in frontal delta power correlated with an increase in lateralized posterior alpha suppression later in the trial, while in trials where the first template was presented lateralized (green line) the lateralized correlation went in the opposite direction (575–850 ms,  $P < 0.05$ , cluster corrected).

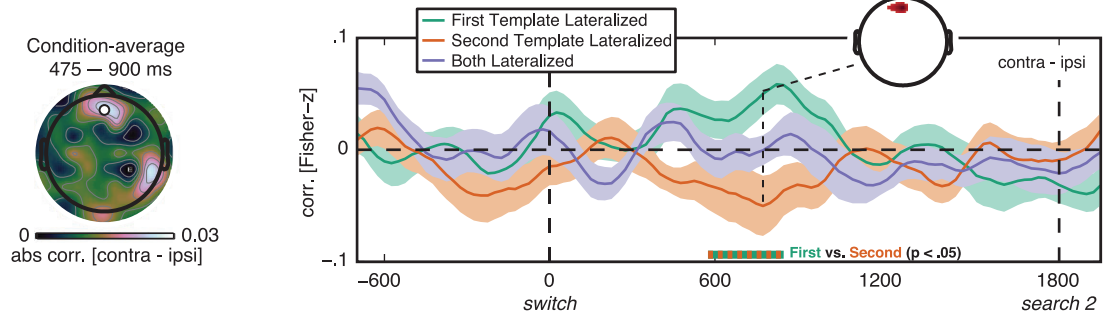
This simple correlation analysis revealed a possible functional linkage between frontal delta and parieto-occipital alpha oscillatory power. Next, we performed an additional analysis to test whether phase–amplitude coupling (PAC) might be the mechanism by which communication between frontal and posterior regions takes place (see online Supplementary Material). Interestingly, our PAC analysis indeed provides subtle evidence for this (Fig. S1). Specifically, prioritization of the second template resulted in stronger coupling between the phase of frontal oscillations at 3 Hz, and the amplitude of posterior alpha contralateral to that item. In contrast, de-prioritization of the first template resulted in weaker coupling between frontal delta and contralateral posterior alpha, resulting in a subtle condition difference between First Template Lateralized and Second Template Lateralized at 3 Hz ( $P = 0.005$ , uncorrected).

Last, we tested whether the increase in frontal delta power also predicted performance on the second search task. Indeed, the condition-average delta power in frontal electrodes showed a robust negative correlation with the reaction time on the

## A Condition-average frontal delta power



## B Correlation: frontal delta power - lateralized posterior alpha power



## C Condition-average correlation: frontal delta power - reaction time search 2

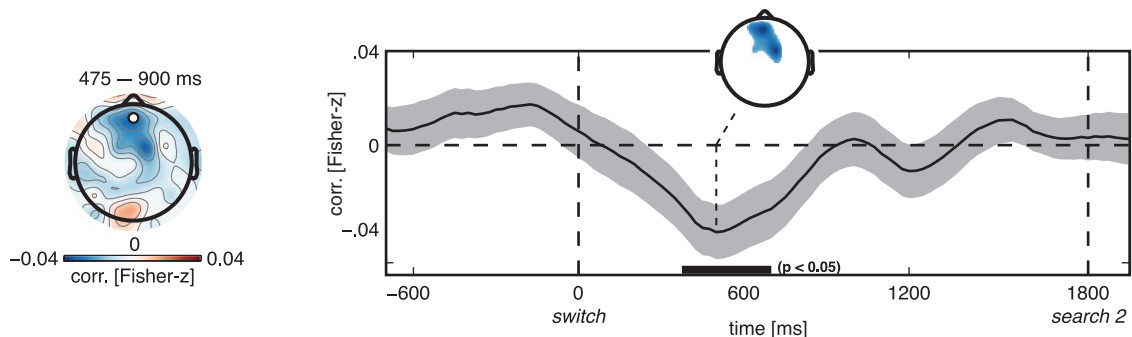


**Figure 5.** Frontal delta power exerts top-down control during priority switch in VWM. (A) Condition-average frontal delta/low-theta (hereafter: delta) power. The topography illustrates delta power averaged over the time-frequency cluster indicated by the black outline in the time-frequency plot. The time-frequency plot illustrates power at an average of AFz/3/4, Fz/1/2 and FCz/1/2 (black-bordered white disks in topography) during the second delay period. Only data from the trials where the first search display was absent (40% of all trials) are depicted in this figure, and activity is time-locked to the auditory switch cue. The black outline indicates power significantly different from baseline at  $P < 0.001$ , cluster corrected. The black horizontal dotted line within the cluster indicates which part of the cluster (i.e., above 2 Hz, see main text subsection Electrode, Frequency and Time Window Selection) was used for all subsequent analyses involving frontal delta power. (B) Single-trial correlation between frontal delta power (at example electrode AFz as indicated with disc in the topography on the left, and averaged over the significant time-frequency cluster in panel a) and lateralized posterior alpha power (electrodes and frequency range as in Fig. 4B), calculated per time point. Memory display conditions are indicated by color as in Figures 3B and 4B. The topography in the left column shows absolute condition-average correlation values. (C) Within-subject condition-average correlation between frontal delta power (at example electrode AFz, frequency range as in the cluster in panel a) and the reaction time on the second search task. In every time series plot, the lines and shaded areas denote subject mean and standard error of the mean for normalized data, respectively. Horizontal double-colored (B) and black (C) thick lines on the x-axis illustrate the time points with a significant condition-difference (B) or a significant difference from zero (C) after cluster correction at  $P < 0.05$ , for the example electrodes used for the time series plots (see main text subsection Results for complete time intervals of the significant clusters). The colored data in the small inset topographies in (B) and (C) indicate which electrodes were part of the significant cluster ( $P < 0.05$ ) for the condition difference (B) or the condition average (D) at an example time point indicated by the dashed line. The time intervals selected for the large topographies in the left column in b and c were selected for illustrative purposes. Importantly, for panel C all time-points and all 64 electrodes were included in the permutation test. For panel B, only the 9 a priori selected frontal electrodes were included in the permutation test.

second search task (375–1225 ms,  $P < 0.05$ , cluster corrected). In other words, trials with stronger switch-cue-related delta power were also trials where the second target was found more rapidly during the subsequent search.

A potential caveat of the observed delta-response is that stimulus-evoked event-related potentials (ERPs) often manifest in transient power increases in the low frequency range. Thus,

the stimulus-evoked response to the auditory cue could have spuriously driven our delta findings. Although this would not explain the specific relationship to lateralized posterior effects, we nevertheless decided to run a control analysis, in which we performed all the above reported correlation analyses with the auditory cue-related potential in the broadband EEG (see online Supplementary Material). The results clearly deviated from the

above-mentioned patterns of correlation with frontal delta power, in that there were neither significant condition differences in delta-alpha correlation, nor were there significant correlations for any of the individual conditions. Similarly, the ERP did not correlate with behavior during the time interval in which delta power did. Thus, we believe that our frontal signal of interest is best described as low-frequency oscillatory activity, rather than a cue-evoked ERP.

In sum, our results reveal an important role for the modulation of frontal delta and lateralized posterior alpha oscillatory activity. Specifically, from the moment at which subjects could drop the first template in favor of prioritizing the second template, a switch in lateralized cross-frequency coupling ensued that was remarkably similar to the switch observed in local posterior alpha lateralization. Furthermore, the frontal delta power increase that accompanied the switch predicted performance after the switch. These results thus support the idea that frontal delta oscillations are important in the top-down control of goal-driven priority changes within VWM.

## Discussion

We investigated the oscillatory dynamics that underlie one of the key characteristics of a flexible visual working memory system: keeping multiple items in memory while only assigning priority to the item that is relevant for the current perceptual goal, and “switching gears” to a memory item that was hitherto prospectively relevant, for a subsequent perceptual goal. We measured EEG while observers memorized two items, a current target and a prospective target representation for two consecutive search tasks. First, although our behavioral results indicated that both these target representations were encoded equally well, hemisphere-specific posterior alpha suppression during encoding and initial maintenance was stronger for current compared with prospective targets, indeed reflecting differences in their state of initial task relevance. Second, a cognitive switch between memory representations was reflected in a neural switch: when a former target representation could be dropped in favor of a prospective (and thus now current) representation, lateralized alpha suppression flipped across hemispheres. This further supports the notion that alpha-band activity in memory continues to serve as a spatially-specific attentional gating mechanism, yet within visual working memory and driving the de- as well as the re-activation of items according to the task structure. Third, we uncovered the putative top-down drive of this switching between representations, in that delta oscillations over frontal regions both predicted the switch-related reversal of alpha lateralization, and supported faster target detection in the subsequent search task.

### Alpha-Band Suppression Supports Current Priority Status of Visual Working Memory Representations

The initial encoding phase and the following first retention interval exhibited robust parieto-occipital alpha suppression, which was stronger contralateral compared with ipsilateral to the memory items. Such a lateralized difference in alpha suppression has been found before, both during visual attention to anticipated target locations (Sauseng et al. 2005b; Thut et al. 2006; Spaak et al. 2015; Wildegger et al. 2017), and during VWM maintenance (Fukuda et al. 2015; Myers et al. 2015b; Schneider et al. 2015, 2016; van Driel et al. 2017). Posterior alpha lateralization during working memory maintenance presumably serves

to control the spatiotopic access to recently encoded relevant visual information (Myers et al. 2015b), which can subsequently be processed further in object-selective cortex (Zumer et al. 2014). Here, lateralized alpha suppression was stronger for prioritized working memories needed for the task at hand, compared with prospective memories needed for the later task. Posterior alpha lateralization thus does not merely reflect processing of relevant visual information, but its relative strength dissociates between the relative priority of multiple representations simultaneously held in working memory (de Vries et al. 2017; van Ede 2017). Our behavioral results show that this prioritization occurred without a necessary loss of performance, and thus presumably information, on the de-prioritized prospective memory, which is in agreement with previous behavioral findings (Myers et al. 2017a). Recent literature emphasizes the importance of prioritization within VWM, as it enables representations to selectively interact with or be protected from our external attention according to their moment-by-moment task relevance (Carlisle and Woodman 2011; Chun 2011; Olivers and Eimer 2011; Olivers et al. 2011; Myers et al. 2017b). It is suggested that on the one hand, prioritized working memories are maintained through sustained neural activity, equivalent to that observed while externally attending to similar visual stimuli; on the other hand, prospective memories are stored in an activity-silent, de-prioritized state, e.g., through synaptic weight changes (Stokes 2015), or short-term potentiation (Erickson et al. 2009). Empirical support for this dissociation in priority states comes from studies using multi-variate decoding of neuroimaging data during VWM maintenance. That is, while the prioritized working memory can be reliably decoded throughout the maintenance period, supporting the notion of activity-based maintenance, decoding accuracy of prospective memories temporarily drops to baseline, only to return to reliable levels once they become task relevant (Lewis-Peacock et al. 2012; LaRocque et al. 2013, 2016; Sprague et al. 2016). Alternatively, sustained activity for the prospective memory might still be present, yet in anterior (i.e., IPS and FEF) rather than posterior regions (Christophel et al. 2018). Another possibility is that the pattern of either activity or responsivity for the prospective representation fundamentally changes compared with that for the prioritized memory. Recent evidence suggests that the representations for currently relevant and prospectively relevant memories become anti-correlated (van Loon et al. 2018; Yu and Postle 2018). Interestingly, some suggest it is in fact the prioritized memory that undergoes a functional transformation towards a task-specific representational state which efficiently guides our imminent behavior (Myers et al. 2017a), for example by acting as an input filter for target detection (Olivers and Eimer 2011; Myers et al. 2015a; Gayet et al. 2017). One limitation of the current study is that the data do not speak to how the representational state of working memories transforms depending on their priority state. However, our results clearly indicate that alpha suppression allows us to track setting up and switching the relative priority of representations serving imminent and future task goals.

### Task-Driven Priority Switch in Visual Working Memory is Reflected in a Switch in Alpha-Band Lateralization

We demonstrate how relative alpha suppression tracks the changes in VWM priority as induced by altered task goals. In addition to a first target template, our participants remembered a second item that was relevant for a second search task.

Within one trial, a new task goal redefined such a prospective memory item to be the new current template, effectively resulting in a switch in priority across templates within VWM. Indeed, the cue that the first search task could be omitted, and consequently that the current target representation could be dropped in favor of prioritizing the former prospective representation, induced a clear re-emergence of alpha suppression for the latter. Given that the order of task relevance of the two working memories was known a priori, our results thus reveal how such an endogenously initiated priority switch is reflected in posterior alpha power modulations. This finding is consistent with recent studies that found an re-emergence of alpha suppression for newly prioritized working memories, as externally triggered by retro-cues (Myers et al. 2015b; Schneider et al. 2015, 2016) or internally, by temporal expectations (van Ede et al. 2017). Here we show that switches in alpha suppression track the representations necessary for planning consecutive tasks.

In addition to alpha suppression, we found lateralized posterior alpha power to also show enhancement effects, in two consecutive time windows: (1) around the expected onset of the first search task for regions contralateral to the prospective template, and (2) after the cue signaling the switch in relevance, for regions contralateral to the former current template, which at that point could be dropped. Alpha power enhancement has been related to the inhibition of information processing (Klimesch et al. 2007; Palva and Palva 2007; Jensen and Mazaheri 2010; Schneider et al. 2017), and as such the two windows of enhanced alpha power can be interpreted as the de-prioritization of a VWM representation that should either not yet (in case of the prospective item), or no longer (in case of the old current item) interact with the perceptual input. An alternative interpretation of the observed alpha enhancement for prospective memories is that it reflects a mechanism to protect against interference, as to stop new and potentially distracting visual information from being processed at that sensory location (Jensen et al. 2002; Bonnefond and Jensen 2012; Payne et al. 2013). Our behavioral results support this interpretation, as responses were slowed when the spatial location of the prospective memory item and that of the first search target overlapped. In our experiment alpha enhancement could thus reflect the protection of prospective representations leading up to the anticipated first search task. Interestingly, although here posterior alpha enhancement was unable to dissociate these two instances of de-prioritization, they are fundamentally different in that the de-prioritization of the prospective memory is only temporary, while the former current template needs to be dropped indefinitely. More research is warranted to investigate whether making a representation prospective (i.e., temporarily irrelevant) recruits similar mechanisms as making an item totally irrelevant, or to what extent these mechanisms may differ.

### Frontal Delta Oscillations Control Priority Switches in Visual Working Memory

Finally, we are the first to demonstrate how the dynamics of fronto-parietal interactions drive the switch in task-driven priority within VWM. We found that the priority-related parieto-occipital alpha dynamics were coupled to both the amplitude and the phase of delta-band activity, in transiently formed fronto-parietal networks. Specifically, when the current task demands required the prioritization of a thus far not relevant working memory, frontal delta power predicted a re-emergence of posterior alpha suppression over regions that recently encoded that item. In addition, we found subtle evidence that

during that time, the phase of frontal delta oscillations at specifically 3 Hz was coupled to the phase of the envelope of posterior alpha power over those same regions. In contrast, when task demands required the de-prioritization of a VWM representation because it was currently irrelevant, frontal delta power predicted alpha enhancement and frontal delta phase showed reduced coupling with posterior alpha power over regions that recently encoded that respective item. Furthermore, frontal delta power predicted faster response times on the search task that followed the internal priority switch. Previous studies observed similar top-down control over posterior alpha oscillations mediated by frontal low-frequency oscillations during visual attention (Mazaheri et al. 2010; Helfrich et al. 2017) and when inhibiting distraction (Janssens et al. 2018). Interestingly, this cross-frequency coupling was absent in children with ADHD (Mazaheri et al. 2010), which supports the notion that it reflects an important neural control mechanism for effective prioritization of information. Moreover, local low-frequency oscillations in frontal regions have been related to executive control in various cognitive tasks, e.g., during the endogenous maintenance of spatial attention (Daitch et al. 2013), and during VWM (Onton et al. 2005; Sauseng et al. 2005a; 2010; Johnson et al. 2017). Specifically related to the goal-dependent priority switch in our experiment, a recent review emphasizes a specific functional role for the frontal cortex in the switch of cognitive resources towards alternative targets for attention, when current goals are deemed no longer relevant (Mansouri et al. 2017). We show how different oscillatory signals in the EEG allow for the moment-by-moment tracking of such goal changes.

### Limitations

One potential caveat here is that the delta frequency range comprises a relatively slow band. We used rather short time windows in our design, and the transitions in alpha lateralization that we report here were fast paced, encompassing less than 3 delta-band cycles. This might not allow for an accurate estimation of time-resolved coupling between the delta and alpha bands. However, previous studies have argued for a functional role of frontal delta oscillations during visual attention (2 Hz; Daitch et al. 2013) and working memory (3 Hz; Onton et al. 2005) in similar task designs. In addition, functional coupling between posterior alpha and frontal delta has been linked to visual perception (2–4 Hz; Helfrich et al. 2017) and visual attention (3–5 Hz; Mazaheri et al. 2010). Likewise, our analyses on phase-amplitude coupling between posterior alpha power and frontal delta phase (see online Supplementary Material) specifically localize the frontal oscillations of interest to around 3 Hz. Furthermore, our control analyses on cue-evoked ERPs indicate that our frontal signal of interest is best described as low-frequency oscillations (see online Supplementary Material). Taken together, we believe that our frontal delta findings are genuine and indeed are functionally involved in priority switches in VWM. A further limitation specific to the cross-frequency connectivity metrics that we applied to our data is that they do not allow for inferences of directionality. However, we found that posterior alpha lateralization correlated with frontal delta power at an earlier time in the trial, which is in accordance with a previous study (Janssens et al. 2018). Moreover, frontal delta power at time of the switch predicted performance later in the trial. Together, these findings suggest that delta oscillations constitute the frequency range with which frontal-to-posterior top-down control can affect posterior alpha oscillations during priority switches within VWM.



## Conclusion

We show that posterior alpha lateralization reliably and consistently dissociates between priority states in VWM. Furthermore, we reveal how the flexible prioritization and de-prioritization of VWM representations, depending on their moment-by-moment task relevance, is tracked by alpha suppression and alpha enhancement over sensory regions that recently encoded those representations. Lastly, we provide novel evidence that the brain orchestrates the switch in priority status between multiple VWM representations by means of a large-scale functional network in which frontal delta oscillations exert top-down control over posterior alpha oscillations.

## Supplementary Material

Supplementary material is available at *Cerebral Cortex* online.

## Funding

This work was supported by the European Research Council (ERC) Consolidator grant (ERC-2013-2013-CoG-615423) to CNLO.

## Notes

*Conflict of Interest:* The authors declare no competing financial interests.

## References

- Alekseichuk I, Turi Z, De Lara A, Antal A, Alekseichuk I, Turi Z, De Lara GA, Antal A, Paulus W. 2016. Spatial working memory in humans depends on theta and high gamma synchronization in the prefrontal cortex article spatial working memory in humans depends on theta and high gamma synchronization in the prefrontal cortex. *Curr Biol*. 26: 1513–1521.
- Bonnefond M, Jensen O. 2012. Alpha oscillations serve to protect working memory maintenance against anticipated distracters. *Curr Biol*. 22:1969–1974.
- Bundesden C. 1990. A theory of visual attention. *Psychol Rev*. 97: 523–547.
- Buzsáki G, Draguhn A. 2004. Neural oscillations in cortical networks. *Sci*. 304: 1926–1929.
- Canolty RT, Knight RT. 2010. The functional role of cross-frequency coupling. *Trends Cogn Sci*. 14:506–515.
- Carlisle NB, Woodman GF. 2011. Automatic and strategic effects in the guidance of attention by working memory representations. *Acta Psychol (Amst)*. 137:217–225.
- Christophel TB, Iamshchinina P, Yan C, Allefeld C, Haynes JD. 2018. Cortical specialization for attended versus unattended working memory. *Nat Neurosci*. 21:494–496.
- Chun MM. 2011. Visual working memory as visual attention sustained internally over time. *Neuropsychologia*. 49: 1407–1409.
- Cohen MX. 2014. *Analyzing Neural Time Series Data: Theory and Practice*. Cambridge, MA: MIT Press.
- Cousineau D. 2005. Confidence intervals in within-subject designs: a simpler solution to Loftus and Masson's method. *Tutor Quant Methods Psychol*. 1:42–45.
- Daitch AL, Sharma M, Roland JL, Astafiev SV, Bundy DT, Gaona CM, Snyder AZ, Shulman GL, Leuthardt EC, Corbetta M. 2013. Frequency-specific mechanism links human brain networks for spatial attention. *Proc Natl Acad Sci*. 110: 19585–19590.
- de Vries IEJ, van Driel J, Olivers CNL. 2017. Posterior alpha EEG dynamics dissociate current from future goals in working memory guided visual search. *J Neurosci*. 37:2945–16.
- Delorme A, Makeig S. 2004. EEGLAB: an open source toolbox for analysis of single-trial EEG dynamics including independent component analysis. *J Neurosci Methods*. 134:9–21.
- Derrington AM, Krauskopf J, Lennie P. 1984. Chromatic mechanisms in lateral geniculate nucleus of macaque. *J Physiol*. 357:241–265.
- Desimone R, Duncan J. 1995. Neural mechanisms of selective visual attention. *Annu Rev Neurosci*. 18:193–222.
- Duncan J, Humphreys GW. 1989. Visual search and stimulus similarity. *Psychol Rev*. 96:433–458.
- Erickson MA, Maramba LA, Lisman J. 2009. A single brief burst induces GluR1-dependent associative short-term potentiation: a potential mechanism for short-term memory. *J Cogn Neurosci*. 22:2530–2540.
- Fukuda K, Mance I, Vogel EK. 2015.  $\alpha$  Power modulation and event-related slow wave provide dissociable correlates of visual working memory. *J Neurosci*. 35:14009–14016.
- Fuster J. 2001. The prefrontal cortex – an update. Time is of the essence. *Neuron*. 30:319–333.
- Gayet S, Guggenmos M, Christophel TB, Haynes J-D, Paffen CLE, Van der Stigchel S, Sterzer P. 2017. Visual working memory enhances the neural response to matching visual input. *J Neurosci*. 37:6638–6647.
- Groppe DM, Makeig S, Kutas M. 2009. Identifying reliable independent components via split-half comparisons. *Neuroimage*. 45:1199–1211.
- Gunseli E, Meeter M, Olivers CNL. 2014. Is a search template an ordinary working memory? Comparing electrophysiological markers of working memory maintenance for visual search and recognition. *Neuropsychologia*. 60:29–38.
- Helfrich RF, Huang M, Wilson G, Knight RT. 2017. Prefrontal cortex modulates posterior alpha oscillations during top-down guided visual perception. *Proc Natl Acad Sci*. 114:9457–9462.
- Helfrich RF, Knight RT. 2016. Oscillatory dynamics of prefrontal cognitive control. *Trends Cogn Sci*. 20:916–930.
- Janssens C, De Loof E, Boehler CN, Pourtois G, Verguts T. 2018. Occipital alpha power reveals fast attentional inhibition of incongruent distractors. *Psychophysiology*. 55:e13011.
- Jensen O, Colgin LL. 2007. Cross-frequency coupling between neuronal oscillations. *Trends Cogn Sci*. 11:7–9.
- Jensen O, Gelfand J, Kounios J, Lisman JE. 2002. Oscillations in the alpha band (9–12 Hz) increase with memory load during retention in a short-term memory task. *Cereb Cortex*. 12: 877–882.
- Jensen O, Mazaheri A. 2010. Shaping functional architecture by oscillatory alpha activity: gating by inhibition. *Front Hum Neurosci*. 4:186.
- Jensen O, Tesche CD. 2002. Frontal theta activity in humans increases with memory load in a working memory task. *Eur J Neurosci*. 15:1395–1399.
- Johnson EL, Dewar CD, Solbakk AK, Endestad T, Meling TR, Knight RT. 2017. Bidirectional Frontoparietal oscillatory systems support working memory. *Curr Biol*. 27:1829–1835.e4.
- Kayser J, Tenke CE. 2015. On the benefits of using surface Laplacian (current source density) methodology in electrophysiology. *Int J Psychophysiol*. 97:171–173.
- Klimesch W, Sauseng P, Hanslmayr S. 2007. EEG alpha oscillations: the inhibition-timing hypothesis. *Brain Res Rev*. 53: 63–88.
- Lara AH, Wallis JD. 2015. The role of prefrontal cortex in working memory: a mini review. *Front Syst Neurosci*. 9:1–7.

- LaRocque JJ, Lewis-Peacock J a, Drysdale AT, Oberauer K, Postle BR. 2013. Decoding attended information in short-term memory: an EEG study. *J Cogn Neurosci*. 25:127–142.
- LaRocque JJ, Riggall AC, Emrich SM, Postle BR. 2016. Within-category decoding of information in different attentional states in short-term memory. *Cereb Cortex*. 1–10.
- Lewis-Peacock JA, Drysdale AT, Oberauer K, Postle BR. 2012. Neural evidence for a distinction between short-term memory and the focus of attention. *J Cogn Neurosci*. 24:61–79.
- Lopez-Calderon J, Luck SJ. 2014. ERPLAB: an open-source toolbox for the analysis of event-related potentials. *Front Hum Neurosci*. 8:1–14.
- Love J, Selker R, Marsman M, Jamil T, Dropmann D, Verhagen J, Wagenmakers EJ. 2015. JASP (Version 0.7). Computer Software.
- Mansouri FA, Koechlin E, Rosa MGP, Buckley MJ. 2017. Managing competing goals—a key role for the frontopolar cortex. *Nat Rev Neurosci*. 18:645–657.
- Maris E. 2012. Statistical testing in electrophysiological studies. *Psychophysiology*. 49:549–565.
- Maris E, Oostenveld R. 2007. Nonparametric statistical testing of EEG- and MEG-data. *J Neurosci Methods*. 164:177–190.
- Marshall TR, Bergmann TO, Jensen O. 2015. Frontoparietal structural connectivity mediates the top-down control of neuronal synchronization associated with selective attention. *PLoS Biol*. 13:1–17.
- Mathôt S, Schreij D, Theeuwes J. 2012. OpenSesame: an open-source, graphical experiment builder for the social sciences. *Behav Res Methods*. 44:314–324.
- MATLAB Release. 2014. The MathWorks, Inc., Natick, Massachusetts, United States.
- Mazaheri A, Coffey-Corina S, Mangun GR, Bekker EM, Berry AS, Corbett BA. 2010. Functional disconnection of frontal cortex and visual cortex in attention-deficit/hyperactivity disorder. *Biol Psychiatry*. 67:617–623.
- Mazaheri A, Nieuwenhuis ILC, Van Dijk H, Jensen O. 2009. Prestimulus alpha and mu activity predicts failure to inhibit motor responses. *Hum Brain Mapp*. 30:1791–1800.
- Miller EK, Cohen JD. 2001. An integrative theory of prefrontal cortex function. *Annu Rev Neurosci*. 24:167–202.
- Monsell S. 2003. Task switching. *Trends Cogn Sci*. 7:134–140.
- Morey RD. 2008. Confidence intervals from normalized data: a correction to Cousineau (2005). *Tutor Quant Methods Psychol*. 4:61–64.
- Myers NE, Chekroud SR, Stokes MG, Nobre AC. 2017a. Benefits of flexible prioritization in working memory can arise without costs. *J Exp Psychol Hum Percept Perform*. 44:398–411.
- Myers NE, Rohenkohl G, Wyart V, Woolrich MW, Nobre AC, Stokes MG. 2015a. Testing sensory evidence against mnemonic templates. *Elife*. 4:e09000.
- Myers NE, Stokes MG, Nobre AC. 2017b. Prioritizing information during working memory: beyond sustained internal attention. *Trends Cogn Sci*. 21:449–461.
- Myers NE, Walther L, Wallis G, Stokes MG, Nobre AC. 2015b. Temporal dynamics of attention during encoding versus maintenance of working memory: complementary views from event-related potentials and alpha-band oscillations. *J Cogn Neurosci*. 27:492–508.
- Oberauer K. 2002. Access to information in working memory: exploring the focus of attention. *J Exp Psychol Learn Mem Cogn*. 28:411–421.
- Olivers CNL, Meijer F, Theeuwes J. 2006. Feature-based memory-driven attentional capture: visual working memory content affects visual attention. *J Exp Psychol Hum Percept Perform*. 32:1243–1265.
- Olivers CNL, Peters J, Houtkamp R, Roelfsema PR. 2011. Different states in visual working memory: when it guides attention and when it does not. *Trends Cogn Sci*. 15:327–334.
- Olivers CNL, Eimer M. 2011. On the difference between working memory and attentional set. *Neuropsychologia*. 49:1553–1558.
- Onton J, Delorme A, Makeig S. 2005. Frontal midline EEG dynamics during working memory. *Neuroimage*. 27:341–356.
- Oostenveld R, Fries P, Maris E, Schoffelen JM. 2011. FieldTrip: open source software for advanced analysis of MEG, EEG, and invasive electrophysiological data. *Comput Intell Neurosci*. 2011:156869.
- Palva S, Palva JM. 2007. New vistas for  $\alpha$ -frequency band oscillations. *Trends Neurosci*. 30:150–158.
- Paneri S, Gregoriou GG. 2017. Top-down control of visual attention by the prefrontal cortex. functional specialization and long-range interactions. *Front Neurosci*. 11:1–16.
- Payne L, Guillory S, Sekuler R. 2013. Attention-modulated alpha-band oscillations protect against intrusion of irrelevant information. *J Cogn Neurosci*. 25:1463–1476.
- Perrin F, Pernier J, Bertrand O, Echallier JF. 1989. Spherical splines for scalp potential and current density mapping. *Electroencephalogr Clin Neurophysiol*. 72:184–187.
- Romei V, Gross J, Thut G. 2010. On the role of prestimulus alpha rhythms over occipito-parietal areas in visual input regulation: correlation or causation? *J Neurosci*. 30:8692–8697.
- Rouder JN, Speckman PL, Sun D, Morey RD, Iverson G. 2009. Bayesian t tests for accepting and rejecting the null hypothesis. *Psychon Bull Rev*. 16:225–237.
- Sauseng P, Griesmayr B, Freunberger R, Klimesch W. 2010. Control mechanisms in working memory: a possible function of EEG theta oscillations. *Neurosci Biobehav Rev*. 34:1015–1022.
- Sauseng P, Klimesch W, Schabus M, Doppelmayr M. 2005a. Fronto-parietal EEG coherence in theta and upper alpha reflect central executive functions of working memory. *Int J Psychophysiol*. 57:97–103.
- Sauseng P, Klimesch W, Stadler W, Schabus M, Doppelmayr M, Hanslmayr S, Gruber WR, Birbaumer N. 2005b. A shift of visual spatial attention is selectively associated with human EEG alpha activity. *Eur J Neurosci*. 22:2917–2926.
- Schneider D, Barth A, Haase H, Hickey C, Wascher E. 2017. Distractor inhibition contributes to retroactive attentional orienting within working memory: Evidence by lateralized event-related parameters of the EEG. *bioRxiv*.
- Schneider D, Mertes C, Wascher E. 2015. On the fate of non-cued mental representations in visuo-spatial working memory: evidence by a retro-cuing paradigm. *Behav Brain Res*. 293:114–124.
- Schneider D, Mertes C, Wascher E. 2016. The time course of visuo-spatial working memory updating revealed by a retro-cuing paradigm. *Sci Rep*. 6:21442.
- Siegel M, Donner TH, Engel AK. 2012. Spectral fingerprints of large-scale neuronal interactions. *Nat Rev Neurosci*. 13:20–25.
- Silver NC, Dunlap WP. 1987. Averaging correlation coefficients: should Fisher's z transformation be used? *J Appl Psychol*. 72:146–148.
- Spaak E, Fonken Y, Jensen O, de Lange FP. 2015. The neural mechanisms of prediction in visual search. *Cereb Cortex*. 26:1–10.
- Sprague TC, Ester EF, Serences JT. 2016. Restoring latent visual working memory representations in human cortex. *Neuron*. 91:694–707.
- Stokes MG. 2015. 'Activity-silent' working memory in prefrontal cortex: a dynamic coding framework. *Trends Cogn Sci*. 19:394–405.

- Thut G, Nietzel A, Brandt SA, Pascual-Leone A. 2006. Alpha-band electroencephalographic activity over occipital cortex indexes visuospatial attention bias and predicts visual target detection. *J Neurosci.* 26:9494–9502.
- van Driel J, Günseli E, Meeter M, Olivers CNL. 2017. Local and interregional alpha EEG dynamics dissociate between memory for search and memory for recognition. *Neuroimage.* 149:114–128.
- van Ede F. 2017. Mnemonic and attentional roles for states of attenuated alpha oscillations in perceptual working memory: a review. *Eur J Neurosci.* doi:10.1111/ejn.13759.
- van Ede F, Niklaus M, Nobre AC. 2017. Temporal expectations guide dynamic prioritization in visual working memory through attenuated  $\alpha$  oscillations. *J Neurosci.* 37:437–445.
- van Loon AM, Fahrenfort JJ, Olivers CNL. 2018. Current and future goals are represented in opposite patterns in object-selective cortex. *bioRxiv.*
- Wagenmakers E-J, Marsman M, Jamil T, Ly A, Verhagen J, Love J, Selker R, Gronau QF, Šmíra M, Epskamp S, et al. 2017. Bayesian inference for psychology. Part I: theoretical advantages and practical ramifications. *Psychon Bull Rev.* 25:35–57.
- Wildegger T, van Ede F, Woolrich M, Gillebert CR, Nobre AC. 2017. Preparatory alpha-band oscillations reflect spatial gating independently of predictions regarding target identity. *J Neurophysiol.* 117:1385–1394.
- Wolfe JM. 1994. Guided Search 2.0 A revised model of visual search. *Psychon Bull Rev.* 1:202–238.
- Woodman GF, Arita JT. 2011. Direct electrophysiological measurement of attentional templates in visual working memory. *Psychol Sci.* 22:212–215.
- Yu Q, Postle BR. 2018. Different states of priority recruit different neural codes in visual working memory. *bioRxiv.*
- Zumer JM, Scheeringa R, Schoffelen JM, Norris DG, Jensen O. 2014. Occipital alpha activity during stimulus processing gates the information flow to object-selective cortex. *PLoS Biol.* 12:e1001965.